JOURNAL OF MATERIALS SCIENCE 19 (1984) 1699–1709

Energy absorption in blends of polycarbonate with ABS and SAN

T. KURAUCHI, T. OHTA
Toyota Central Research and Development Laboratories, Inc., Nagakute-cho, Aichi-gun, Aichi-ken, Japan

Polycarbonate and its blends with ABS and SAN were tested to study the energy absorbing properties and the deformation mechanism. In tension and impact tests, these blends were found to possess a high energy absorbing capability, high yield strength and large rupture elongation. ABS and SAN particles in the blends deform in a ductile manner to an elongation of more than 100% under a tensile stress. In an elongation test of ABS under a hydraulic pressure of 90×10^5 N m^{-2}, the transformation from crazing to a cold-drawing mechanism was found to occur. The large elongation of ABS and SAN in the blends is attributed to the cold drawing which occurs under the influence of the pressure acting on the dispersed ABS and SAN, caused by the difference between the elastic moduli of the dispersoid and the matrix.

1. Introduction

Most plastics deform in a ductile manner, and they absorb much energy. This energy absorbing property attracts much interest in their application to protect a driver from injury in traffic accidents. However, a simple analysis reveals that the capability of absorbing the energy is not enough for that purpose. Therefore, some improvement of the property is needed for the application.

Blending of plastics is a well known phenomenon used to improve the mechanical and rheological properties. The technique is expected to be useful for improvement of the energy absorbing capability.

The mechanical behaviour of blends composed of grafted rubbery particles and brittle polymers, such as polystyrene (PS) and styrene acrylonitrile (SAN), has been the subject of intensive research [1–3] and some of them have recently been reviewed by Bucknall [4]. The improved toughness of high impact polystryene (HIPS) and acrylonitrile butadiene styrene (ABS) is thought to be caused by the grafted polybutadiene particles acting as both craze initiators and terminators.

It is interesting to study the energy absorbing property and the deformation behavior of incompatible blends composed of a brittle material (PS, SAN) as a dispersed particle phase and a ductile matrix [polycarbonate (PC), poly(vinyl chloride) (PVC)]. Petrich [5] investigated and interpreted the toughening mechanism of PVC containing MBS (methacrylate–butadiene–styrene) as the result of dilatative lowering of the yield stress of the matrix surrounding the rubber particles, but in his report, the compatibility of the blend components was not clarified. Groeninckx *et al.* [6], recently suggested two deformation mechanisms, crazing and shear-banding, on the tensile behaviour of a blend composed of PC as a matrix and PS as a dispersoid. Their result was, however, limited only to the temperature range between the glass transition temperatures of the two constituents.

The aim of the present research is to study blending of polycarbonate (PC) with ABS and SAN and the mechanical properties, especially the energy absorbing property of the blends.

2. Experimental details

Specimens were made by blending SAN and two kinds of ABS, Styrac and Sevian, with PC. These raw plastics are all commercially available; PC (Eupilon S-3000, Mitsubishi Gas Chemical Co.),

0022–2461/84 $03.00 + .12

TABLE I Chemical compositions and molecular weights of raw materials

Resin	Content		
	Molecular weight	Acrylonitrile	Butadiene
PC	3.5×10^4		
Styrac ABS		22%	29%
Sevian ABS		20%	37%
SAB	1.78×10^5	50%	

SAN (SAN-H, Asahi Dow Co.), Styrac ABS (Styrac 301, Asahi Dow Co.) and Sevian ABS (Sevian V-300, Diesel Co.). Their chemical compositions as well as their molecular weights are given in Table I. The composition of the blends was widely varied from 10/90 to 90/10 in weight ratio. The blends were prepared in the form of pellets by using a conventional twin-screw extruder at the temperature of 230° C. And these blends were moulded with an injection moulding machine into ASTM D-1822 Type L tensile specimen and rectangular bars for impact testing. The moulding temperature is selected to be 230° C.

The specimens were submitted to a tensile test, a compressive test and a Charpy impact test. The tensile test was carried out by the use of an Instron testing machine, at the crosshead speed of 10 mm min^{-1}. To determine the local elongation of the specimen under the tensile stress, several lines were printed on the surface of the specimen. The temperature in the course of a test was controlled so that it remained constant. The accuracy of control was within ± 2° C. The test temperature was varied from 25 to 100° C. An ASTM D-1822 Type L tensile specimen was used for the test. The compressive test was carried out on an Instron testing machine, with a crosshead speed of 1 mm min^{-1}, at room temperature. The dimension of the specimen for the test was 12 mm × 12 mm × 6 mm. Charpy impact test was performed using a 50 J (5 kg m) capacity machine. The temperature in the test was varied from −40 to 80° C. The dimension of the specimen was 6.4 mm × 12.7 mm × 55 mm and standard notches (ASTM D-256) were cut in these specimens. The unsupported span was 40 mm.

The specimens for these tests were made by injecting the blends into the mould which had dimensions which were a little larger than those of the specimen.

Measurements of the dynamic loss tangents were made by the use of a viscoelastic meter (Iwamoto Manufacture Co.) in the temperature range from 25 to 200° C. The specimens with dimensions of 2 mm × 3 mm × 30 mm were made by punching out the peripheries of the injected blends.

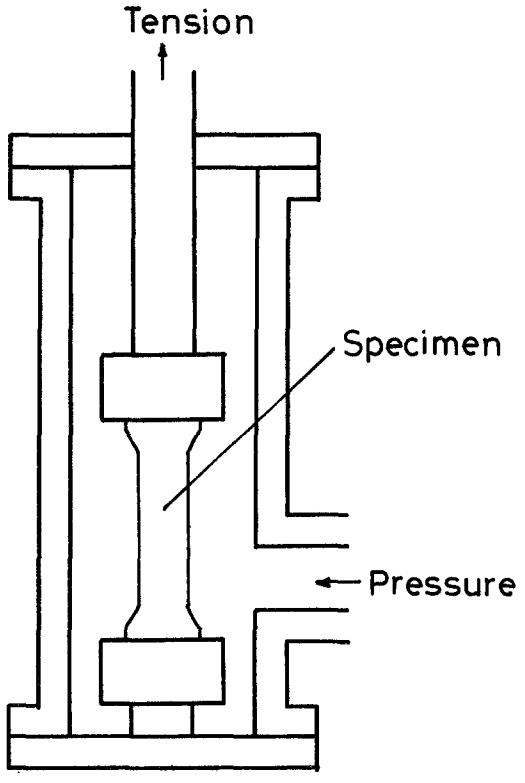

Figure 1 Apparatus for a tensile test under hydraulic pressure.

Also a tensile test under high pressure was made. The apparatus for the test is shown in Fig. 1. The hydraulic pressure can be elevated to 200×10^5 N m^{-2} by the use of machine oil. The pressure medium, machine oil, was selected because it is nonreactive with SAN and ABS. The tensile test was performed with a crosshead speed of 10 mm min^{-1}, at room temperature.

Electron microscopic observation of the specimen, before and after the tensile test, was also performed. For the observation, the specimen containing ABS was stained with osmic acid. Some of the specimens without polybutadiene, or containing SAN and PC only, were modified by adding a small amount of organic metal to the blends in order to observe the samples, since SAN can not be stained with osmic acid. The modification with the organic metal was made by mixing zinc steric acid with SAN before blending.

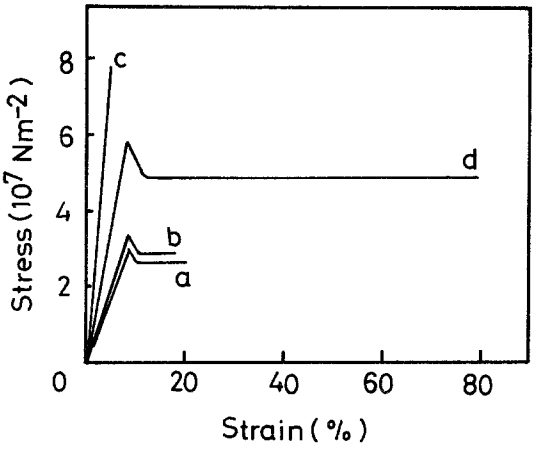

Figure 2 Tensile stress–strain curves of each single phase system; (a) Styrac ABS, (b) Sevian ABS, (c) SAN and (d) PC.

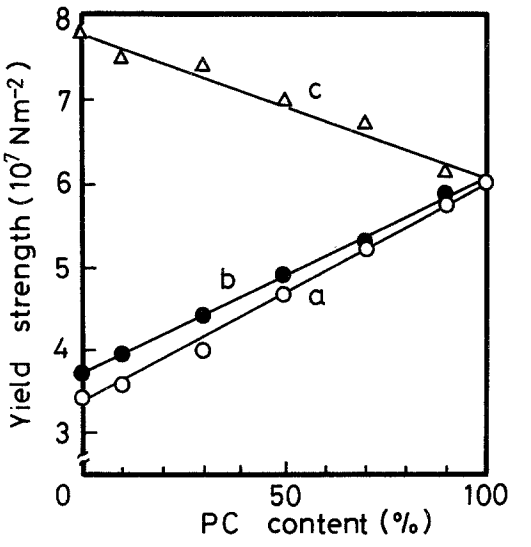

Figure 4 Yield strength of the blends; (a) Styrac ABS–PC, (b) Sevian ABS–PC and (c) SAN–PC.

3. Results and discussions

The stress–strain curves of each single phase system, Styrac ABS, Sevian ABS, SAN and PC, are given in Fig. 2. Typical examples of the curves of the blends, Styrac ABS 30%–PC 70%, Sevian ABS 30%–PC 70%, and SAN 30%–PC 70%, are shown in Fig. 3. As shown in the figures, the SAN polymer is brittle and elongations of ABS polymers are not as large as that of PC. The blends composed of such polymers, however, behave highly ductile under a tensile load, except Sevian ABS 30%–PC 70%. The yield strength, or the ultimate tensile stress, rupture elongation and absorbed energy determined from the stress–strain curves for each of the blends are given in Figs. 4, 5 and 6. In Fig. 4, the fracture strength is plotted instead of the ultimate stress of SAN, as SAN fails without giving the ultimate tensile stress. As shown in the figure, the yield strength of each blend varies linearly with the concentration of PC. The blend of SAN and PC possesses a higher yield strength than PC. The rupture elongation and the absorbed energy of the blends depend much on the nature of ABS as well as the concentration of PC, as shown in Figs. 5 and 6.

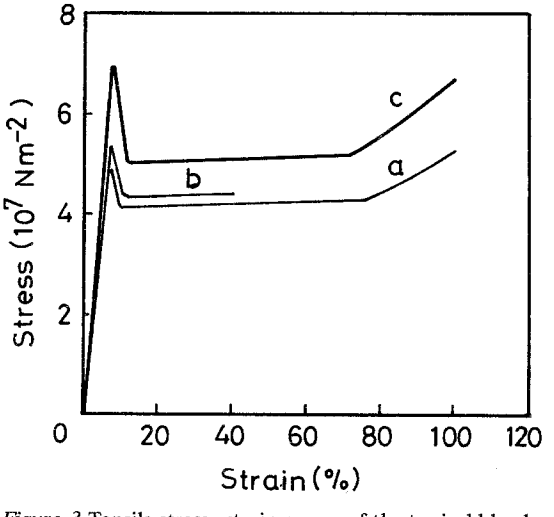

Figure 3 Tensile stress–strain curves of the typical blends; (a) Styrac ABS 30%–PC 70%, (b) Sevian ABS 30%–PC 70% and (c) SAN 30%–PC 70%.

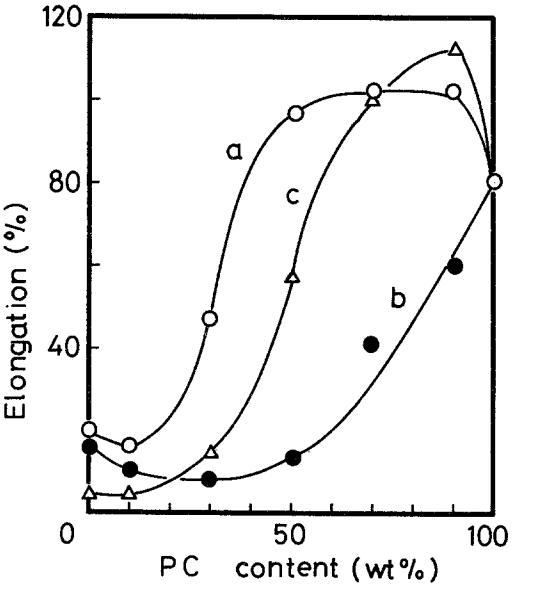

Figure 5 Rupture elongation of the blends; (a) Styrac ABS–PC, (b) Sevian ABS–PC and (c) SAN–PC.

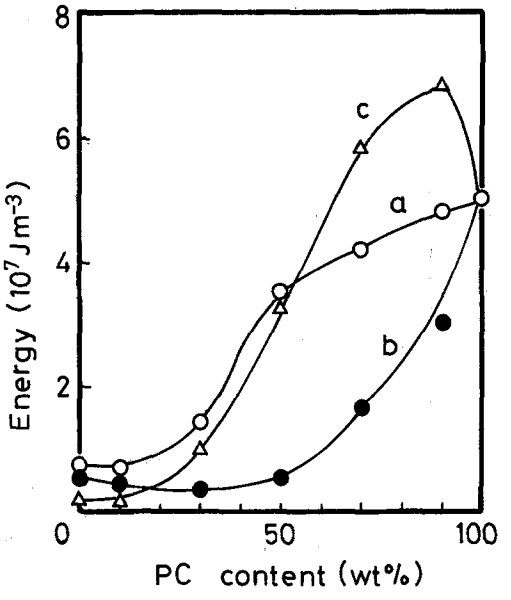

Figure 6 Absorbed energy determined from the tensile stress–strain curves of the blends; (a) Styrac ABS–PC, (b) Sevian ABS–PC and (c) SAN–PC.

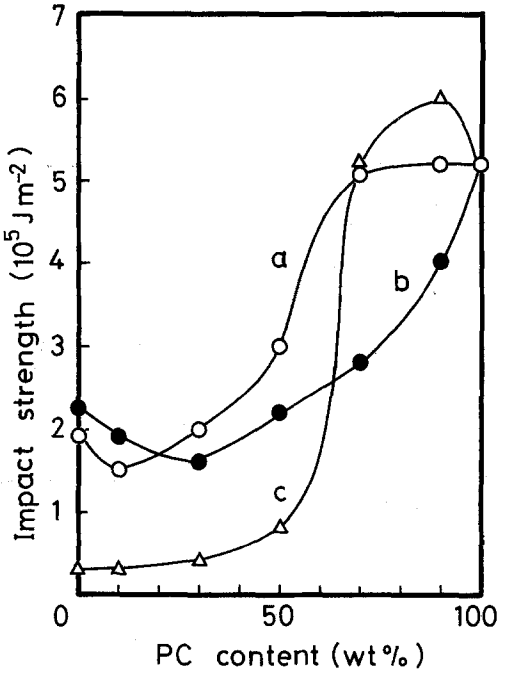

Figure 7 Un-notched impact strength of the blends; (a) Styrac ABS–PC, (b) Sevian ABS–PC and (c) SAN–PC.

In Styrac ABS–PC blends and SAN–PC blends, the elongation and the absorbed energy increases with the concentration of PC, above about 30% PC. The largest elongation is about 100%, which is a little higher than that (80%) of the single phase polymer, PC. Also the largest value of the absorbed energy of some blend is higher than that of PC. In Sevian ABS–PC blend, however, they increase with that of PC only above about 70% of PC.

The un-notched impact strength of each blend is plotted against the composition of the blend, see Fig. 7. The notched impact strength of the blend of a typical composition containing 70% PC and that of 100% PC is plotted against temperature in Fig. 8.

The blend, Styrac 30%–PC 70%, possesses higher impact strength than PC at low temperature, as shown in Fig. 8, and it possesses the same failure elongation and the same energy absorbing capability as PC, as shown in Figs. 5 and 6. However, some of the blends composed of ABS or SAN and PC are proved to be superior to the single phase polymer, PC, which possesses the largest failure elongation and the highest energy absorbing capability in single phase polymers.

The elongation of two kinds of the blend, Styrac ABS–PC and Sevian ABS–PC, differs much from that of each other. The difference in the elongation causes that in the absorbed energy.

The dynamic loss tangent of Styrac ABS–PC is plotted against temperature in Fig. 9. That of Sevian ABS–PC is given in Fig. 10. Dynamic loss tangent has the maximum at the temperature of about 125° C in the Styrac ABS–PC blends. The temperature of 125° C is equal to that at which the maximum of the loss tangent of Styrac ABS

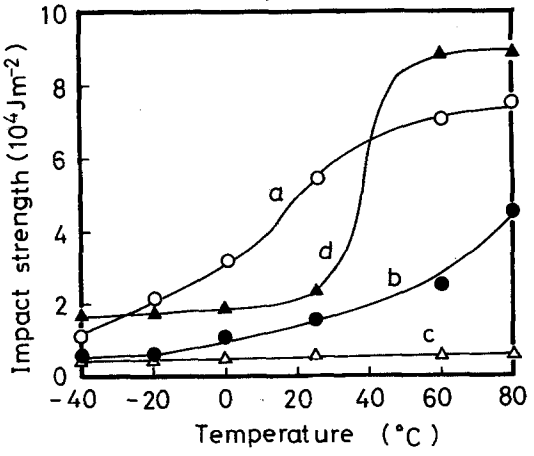

Figure 8 Notched impact strength of the blends is plotted against temperature; (a) Styrac ABS 30%–PC 70%, (b) Sevian ABS 30%–PC 70%, (c) SAN 30%–PC 70% and (d) PC.

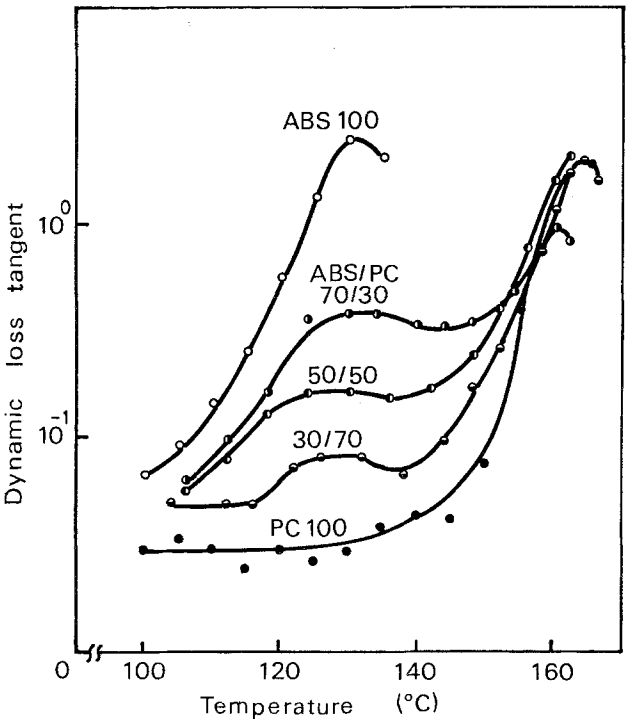

Figure 9 Dynamic loss tangent of Styrac ABS–PC blends.

is given. The curve of the blend approaches to that of PC in high temperature range, as shown in Fig. 9. That of SAN–PC is very similar to that of Styrac ABS–PC blend. A typical example for SAN–PC is shown in Fig. 11. The agreement in the temperatures of the maximum loss tangent and the similarity in the curves suggest that the blend is composed of ABS or SAN and PC in the form of an incompatible mixture. The curve of Sevian ABS–PC blend has the maximum at the temperature of about 125° C. The value of the maximum, however, is small in comparison

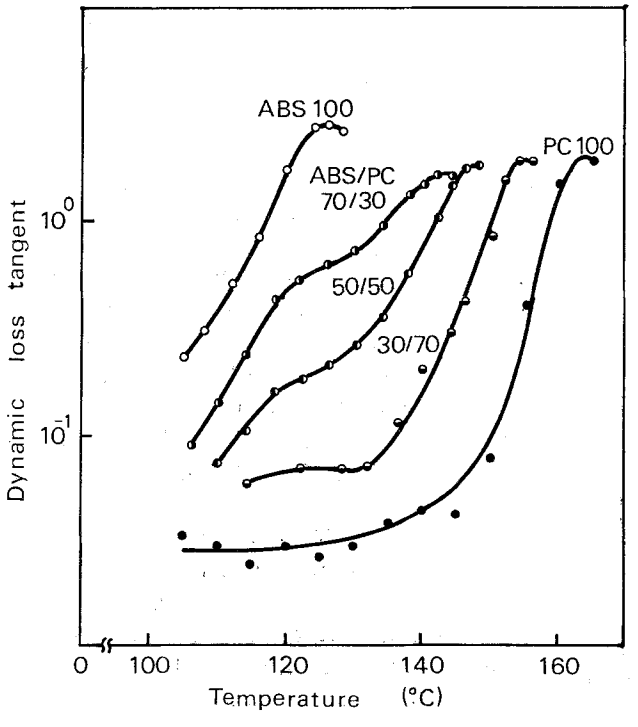

Figure 10 Dynamic loss tangent of Sevian ABS–PC blends.

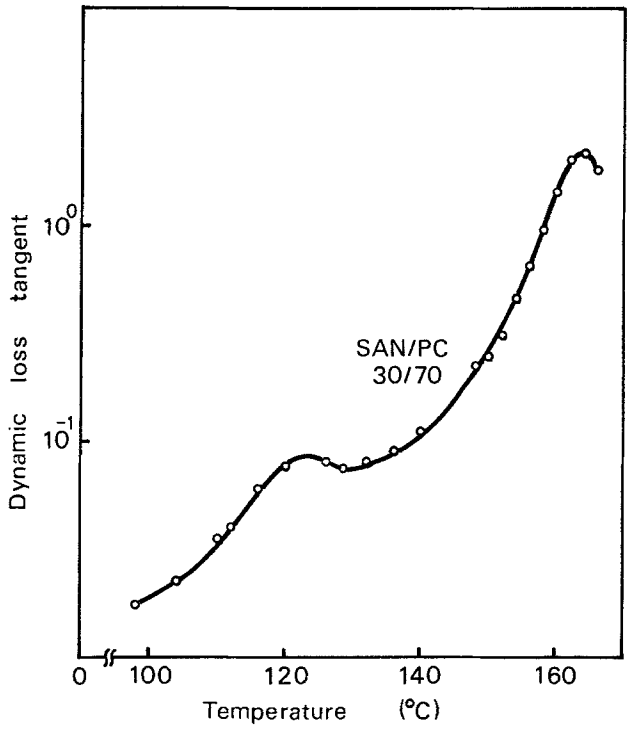

Figure 11 Dynamic loss tangent of the blend, SAN 30%–PC 70%.

with that of Styrac ABS–PC blend. Moreover, the curve does not approach that of PC even in the high temperature range. These suggest that the blend is a compatible mixture. The glass transition temperature of the Sevian ABS–PC blend varies linearly with the concentration of PC, as shown in Fig. 12. The glass transition temperature agrees very well with the calculated one by the use of the Fox equation [7] based on the assumption of compatible mixture of Sevian ABS and PC. These show that the blend, Sevian ABS–PC, is composed of a compatible mixture.

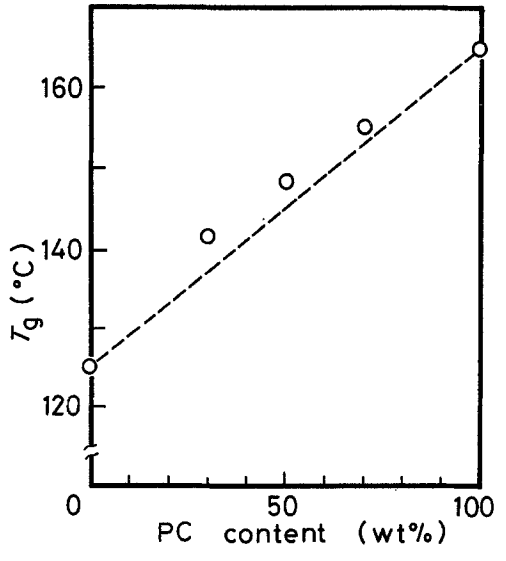

Figure 12 Glass transition temperatures of Sevian ABS–PC blends; (– – – –) calculated by Fox equation and (o) experimentally obtained.

The electron microscopic photographs of the as-blended material are shown in Fig. 13. In the photograph of the blend, Styrac ABS of less than 50%–PC (Fig. 13b), small round structures containing dark particles of diameter 0.2 μm are observed. The same particles are observed also in the polymer, ABS, (see Fig. 13a). The particles are evidently polybutadiene stained with osmic acid. Therefore, the round structure observed in the blend is concluded to be a particle of ABS. From this, it can be concluded that ABS is dispersed in PC as small particles of about 2 μm in diameter in the blend composed of ABS of less than 50% and PC in rest. Also in the SEM photograph of the blend, SAN–PC, small particles of about 1 μm in diameter are observed in the composition range of SAN less than 50%. A typical example is shown in Fig. 13d. The number of particles are shown to increase with the concentration of SAN. Hence, the small particles are concluded to be composed of SAN.

From this, it is concluded that the blends,

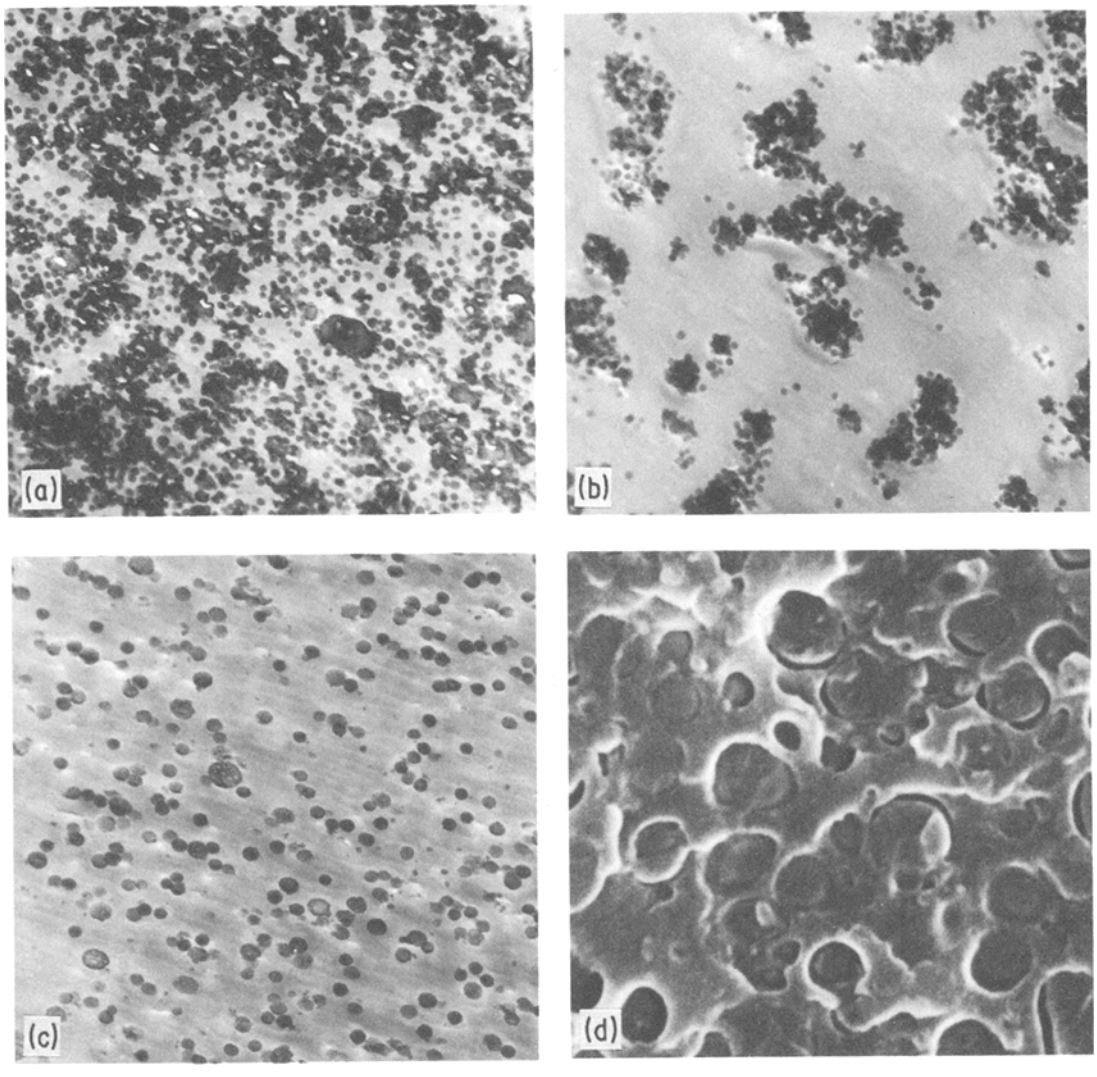

Figure 13 Electron microscopic photographs of the as-blended materials; (a) Styrac ABS, × 5000, (b) Styrac ABS 30%–PC 70%, × 5000, (c) Sevian ABS 30%–PC 70%, × 5000 and (d) SAN 30%–PC 70%, × 10 000.

Styrac ABS–PC and SAN–PC, are composed of ABS particles of about 2 μm in diameter or SAN particles of about 1 μm and PC in the composition of ABS or SAN is less than 50%. The conclusion on the constitution of the blends agrees well with that based on the dynamic loss tangent of the blends. In the blends containing ABS or SAN above 50%, small particles dispersed in matrix are observed. The particles are shown to be composed of PC in the blends. The interchange of the matrix phase and dispersed particle is thought to result from their volume ratio interchange, that is, the major phase forms the matrix and minor phase forms small particles.

The electron microscopic observation of Sevian ABS–PC blends reveals that in the blend dark spots stained with osmic acid, polybutadiene, is dispersed uniformly, as shown in Fig. 13c. This result, based on the measurement of the dynamic loss tangent and the glass transition temperature, supports the conclusion that the blend is composed of a compatible mixture.

In Fig. 14, an election micrograph of the necked part of the blend after the tensile test is shown. As shown in the figure, no crazing is observed in the Styrac ABS–PC and SAN–PC blends. In these blends, the particles, which appeared spherical before testing, are elongated. Elongation of some particles in Styrac ABS 30%–PC 70% blend is more than 100%, and the mean

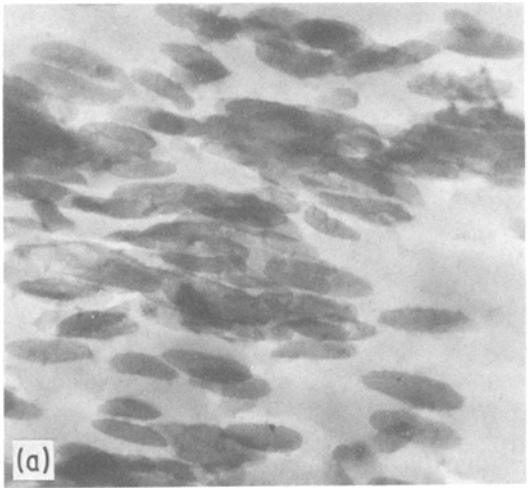

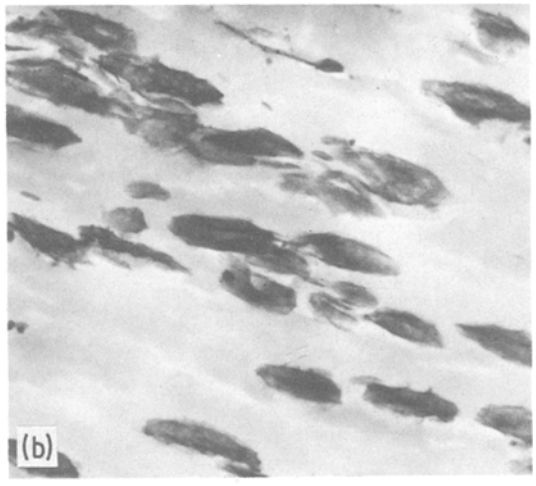

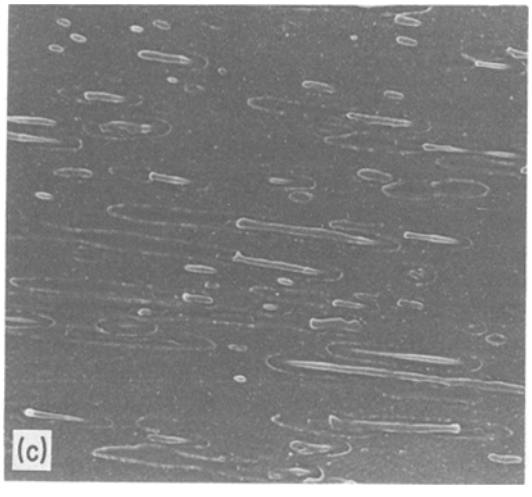

Figure 14 Electron microscopic photographs of the necked part of the blends after a tensile test; (a) Styrac ABS 30%–PC 70%, ×25 000, (b) Sevian ABS 30%–PC 70%, ×25 000 and (c) SAN 10%–PC 90%, ×5000.

elongation is about 100%, which agrees well with the local elongation of the necked part determined from the change of separation between two marks printed on the tensile specimens. The elongation of the particles in SAN 10%–PC 90% blend is about 100% on average, which agrees well with that of the necked part of the specimen. Elongation of some particles is more than 400%, as shown in the figure. These results show that ABS as well as SAN is very ductile in the blend form, in contrast to the low ductility in the single phase polymer.

The high energy absorbing capability of the blends can be attributed partly to the ductility of the ABS particle and the PC matrix. On the assumption that the blend is composed of undeformable particles and a ductile matrix, the absorbed energy of the blend would be much less than that of the matrix polymer, because the energy absorption can be obtained only by the deformable matrix which is smaller in volume fraction than the single phase polymer. The unexpectedly large elongation of SAN in the blend, 400%, shows the occurrence of the large deformability of PC as well, in contrast to the rather small elongation of 80% at most, in the single phase polymer. Therefore, some modification would give a much higher energy absorption for ABS–PC and SAN–PC blends.

In the blend, Sevian ABS–PC, the polybutadiene particles, dispersed uniformly in the as-moulded blend, come to be dispersed non-uniformly in the necked part of the specimen after the tensile test. The separation in the direction parallel to the elongation of the specimen increases after testing, and the separation perpendicular to the elongation decreases slightly. The largest increment in the separation in the parallel direction is nearly the same as the separation before testing for the blend Sevian 30%–PC 70%, which proves that the elongation in the necked part is about 100% at the most. As discussed, the blend is composed of a compatible mixture of ABS and PC, and thus both molecules of ABS and PC are thought to be elongated to about 100% at the most. The average elongation, determined from the marks printed on the specimen, is about 40%. The discrepancy between the elongation values is due to the fact that the large elongation of the blend is limited to a very

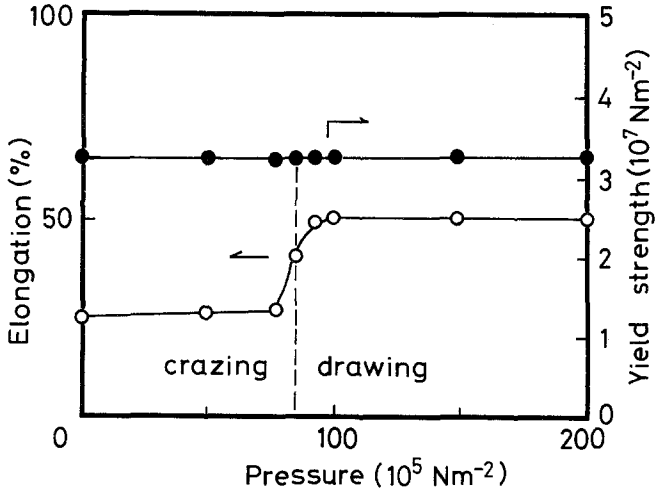

Figure 15 Yield strength and rupture elongation of Styrac ABS under hydraulic pressure.

small area, and most parts of the blend reach failure before reaching an elongation of 100% under the influence of the crack which was initiated from the part which underwent elongation of 100%.

As discussed above, ABS and SAN in the form of a small particle can deform much more than ABS and SAN in single-phase form. The transformation from brittle to ductile in SAN occurs at about 85° C. The assumption of temperature elevation due to the energy absorption in the course of tensile testing would seem to explain the large deformation of SAN and ABS particles in the blends. The absorbed energy, however, is only 50 J cm^{-3} at the most, and the temperature elevation due to the energy is only 40° C at highest. Therefore, the large deformation of SAN and ABS particles can not be attributed to the transformation.

In Fig. 15, the tensile yield strength and rupture elongation of Styrac ABS under hydraulic pressure is plotted against the pressure. As shown in the figure, the rupture elongation of ABS increases rapidly above a pressure of 90×10^5 N m^{-2}. Below this pressure, the material looks translucent or white after the tensile test, which proves that the elongation below this pressure is due to a crazing mechanism. But, above this pressure, it looks transparent, which shows that the large elongation is due to a cold drawing mechanism. The pressure of 90×10^5 N m^{-2} is the transformation pressure from crazing to cold drawing. The manner of the deformation of ABS above the pressure is essentially the same as that below this pressure, that is to say, Young's modulus and yield strength are the same and only the rupture elongation increases rapidly above this pressure.

To understand the large elongation of the blends, the following analysis was tried. The analysis of the elastic stress distribution in a particle-dispersed composite has been made on the following assumptions; (a) dispersed particles are spherical, (b) the interaction among particles is neglected, and (c) the constituents are perfectly bonded together at the interface [8–11]. According to the analysis, stress acts on the equatorial plane of a particle dispersed in a matrix under tensile stress through the differences of Young's modulus and Poisson's ratio between the dispersed sphere (E_2, ν_2) and the matrix (E_1, ν_1). The stress is given as follows:

$$\sigma = [(3\lambda_2 + 2\mu_2)F + 2\mu_2 GM]\epsilon \qquad (1)$$

where

$$M = -\tfrac{1}{3}(1 + \nu_1)$$

$$F = (1 - 2\nu_1)(\lambda_1 + 2\mu_1)/(4\mu_1 + 3\lambda_2 + 2\mu_2)$$

$$G = 15\mu_1(\lambda_1 + 2\mu_1)/[2\mu_2(3\lambda_1 + 8\mu_1) + \mu_1(9\lambda_1 + 14\mu_1)]$$

$$\mu_1 = \frac{E_1}{2(1 + \nu_1)}$$

$$\mu_2 = \frac{E_2}{2(1 + \nu_2)}$$

$$\lambda_1 = \nu_1 E_1/(1 + \nu_1)(1 - 2\nu_1)$$

$$\lambda_2 = \nu_2 E_2/(1 + \nu_2)(1 - 2\nu_2)$$

As discussed above, ABS and SAN are dispersed

in the form of a sphere in PC. By substitution of $E_1 = 170 \times 10^7\ N\,m^{-2}$, $\nu_1 = 0.4$ for PC and $E_2 = 250 \times 10^7\ N\,m^{-2}$, $\nu_2 = 0.35$ for SAN into Equation 1, the following equation is given;

$$\sigma = -1200 \times 10^5 \epsilon \qquad (2)$$

As the values of Young's modulus and Poisson's ratio of ABS, or the system composed of SAN and polybutadiene, are not given, the stress acting in the ABS–PC blend is not known. ABS, however, contains more SAN than polybutadiene, and hence the result given in Equation 2 will be qualitatively useful also for the ABS–PC blend. Equation 2 shows that compressive stress acts on the equatorial plane of the particles in the PC matrix under an applied tensile stress. The value of the compressive stress is evaluated as $24 \times 10^5\ N\,m^{-2}$ for the value of $\epsilon = 0.02$, on the assumption of the elastic limit being more than 0.02. This assumption of the elastic limit will be correct, because the stress–strain curves shown in Fig. 3 appear linear for the strain less than about 0.02. The strain at the yield point is much larger than 0.02, and hence the stress acting on the particles will be much larger than the estimated stress. However the ABS and SAN particles are constrained volumetrically by PC, and are therefore unable to develop the large dilatational strains necessary for significant craze formation in ABS and crack formation in SAN.

According to the results under hydraulic high pressure, ABS deforms in a more ductile manner under a pressure above $90 \times 10^5\ N\,m^{-2}$. Then, the actual value of the compressive stress acting on the ABS and SAN particles will be estimated to be about the same value, $90 \times 10^5\ N\,m^{-2}$. This value can be explained from Equation 2 by substituting $\epsilon = 0.08$, on the assumption that the value, 0.08, can be used as correct for the equation based on the elastic deformation. The value, 0.08, would appear to be too large for the elastic assumption, but for a qualitative discussion it will be not so wrong, as seen in the curves shown in Fig. 3. On this approximation, the large deformation of the blends seems to be understood.

The value of the elongation of the SAN 30%–PC 70% blends, 100%, is yet much larger than the value of ABS under the hydraulic pressure, 50% (Fig. 15). This difference is thought to be attributed to the dimension effect of the specimen. In a small particle, the size of initial flaw is small, and in a large specimen the size would be large.

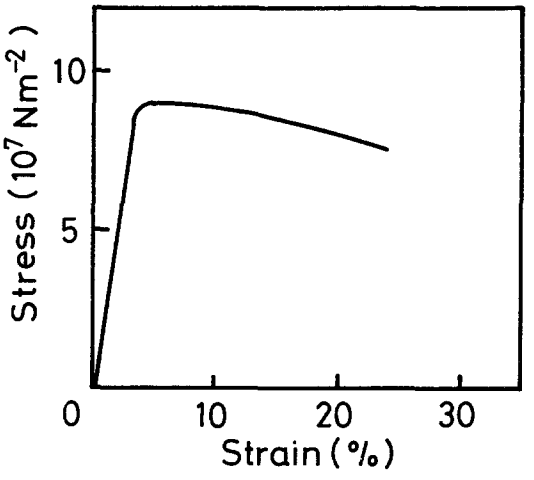

Figure 16 Stress–strain curve of SAN under a compressive test at room temperature.

The large flaw would limit the elongation of SAN in ABS to a small value. The larger strain of PC in the blend, 100%, will be attributed to the intercepting effect of the dispersed ABS and SAN particle against crack propagation in the matrix.

SAN is expected to have a property similar to ABS, because SAN is substantially the same as ABS. However, the transformation from crazing to cold drawing does not occur in SAN, under the hydraulic pressure below $200 \times 10^5\ N\,m^{-2}$. However it behaves as a ductile material under compressive stress, as shown in Fig. 16. Therefore, the absence of the transformation is thought to be only apparent. The lack of dispersed phase (polybutadiene) in the specimen of pure SAN is thought to be a possible reason for the absence of this transformation, as a pinning effect for the propagation of a crack is absent in the specimen. In a small particle, the transformation is expected to occur at the same pressure in SAN, $90 \times 10^5\ N\,m^{-2}$, too. The large elongation of SAN in the blend, SAN–PC, is thought to be attributed also to the compressive stress acting on the SAN particle.

Therefore, the large absorbed energy of the blends is thought to result partly from the large elongation which is caused by tensile stress under the influence of the compressive pressure acting on the dispersed ABS and SAN particles. Moreover, such a large value of absorbed energy is given only in the blend which is composed of dispersed ABS or SAN particles in a continuous ductile material, PC, because the compressive stress occurs only in a blend of such a combination of

materials. This would be the reason why the energy decreases in a blend composed of less PC and more ABS or SAN, in which PC is dispersed in the form of small particles in an ABS or SAN matrix.

The similarity in the deformation manner of ABS above and below the transformation pressure suggests that the deformation mechanism of crazing in ABS is substantially the same as that of cold drawing and that the difference between the two mechanisms lies only in the introduction of elongated voids in the material in crazing. Therefore, cold drawing is expected to occur locally in ABS even under ambient pressure. This would support Bucknall's hypothesis [4] that energy absorption of ABS would be partly due to cold drawing occurring simultaneously with crazing.

4. Conclusions

1. It was confirmed that some blends in the systems, ABS–PC and SAN–PC, possess high energy absorbing capability, high yield strength and large rupture elongation.

2. In the blends, ABS and SAN in the form of particle deform in a ductile manner to the elongation of more than 100% under tensile stress.

3. The occurrence of the transformation from crazing mechanism to cold drawing mechanism in the elongation of ABS at the hydraulic pressure of 90×10^5 N m^{-2} was found.

4. The large elongation of ABS and SAN in the blends is attributed to the cold drawing occurring under the influence of the pressure acting on the dispersed ABS and SAN caused by the difference between the elastic moduli of the dispersoid and the matrix.

Acknowledgement

The authors thank Drs N. Komatsu and O. Kamigaito for their discussion and encouragement throughout this work. Thanks are given also to Mr M. Matsushita for his help in electron microscopic observation of the blends.

References

1. C. B. BUCKNALL and D. CLAYTON, *J. Mater. Sci.* 7 (1972) 202.
2. C. B. BUCKNALL and I. C. DRINKWATER, *ibid.* 8 (1973) 1800.
3. A. M. DONALD and E. J. KRAMER, *ibid.* 17 (1982) 1765.
4. C. B. BUCKNALL, "Toughened Plastics" (Applied Science Publishers, London, 1977).
5. R. P. PETRICH, *Polym. Eng. Sci.* 13 (1978) 248.
6. G. GROENINCKX, S. CHANDRA, H. BERGHMANS and G. SMETS, *Adv. Chem. Ser.* 176 (1979) 337.
7. T. G. FOX, *Bull. Amer. Phys. Soc.* 1 (1956) 123.
8. J. M. DEWEY, *J. Appl. Phys.* 16 (1945) 55.
9. *Idem, ibid.* 18 (1947) 132.
10. *Idem, ibid.* 18 (1947) 578.
11. K. TAKAHASHI, M. IKEDA, K. HARAKAWA and K. TANAKA, *J. Polym. Sci.* 16 (1978) 415.

Received 14 March
and accepted 19 September 1983